



Evaluation of strategies for enhanced bioethanol production from melon peel waste

Xiana Rico^{a,b}, Remedios Yáñez^{a,b,*}, Beatriz Gullón^a

^a Universidade de Vigo, Departamento de Enxeñaría Química, Facultade de Ciencias, As Lagoas, 32004 Ourense, Spain

^b CINBIO, Universidade de Vigo, 36310 Vigo, Spain

ARTICLE INFO

Keywords:

Melon by-products
Bioethanol
Enzymatic hydrolysis
Simultaneous saccharification and fermentation

ABSTRACT

Melon peels can be a low-cost raw material for the production of bioethanol due to its high worldwide production and contents in cellulose, protein and minerals. In this work, several strategies were proposed for this purpose. Centrifugation of the raw material and autohydrolysis of the washed solid were used as pretreatment for the recovery of a sugar rich juice and a glucan rich solid, respectively. The enzymatic hydrolysis of the autohydrolyzed spent solid was studied by response surface assessment. High glucose concentrations (35.15 g/L after 24 h) and yields were obtained operating at a liquid solid ratio of 10 g/g and cellulase to solid ratio of 17.5 FPU/g. In the selected conditions, the simultaneous saccharification and fermentation (SSF) of the solid was studied using the juice (virgin and concentrated) in the formulation of the media. Moreover, the separate fermentation of the juice (virgin and concentrated) was also evaluated, as well as a pre-fermentation followed by SSF. Finally, several scenarios were proposed, achieving the maximum bioethanol production by SSF and separate juice fermentation (17.84 g/100 g melon peel), and the maximum concentration by SSF using concentrated juice in the formulation of the medium (56.24 g/L).

1. Introduction

The negative environmental impact of fossil fuels and their fast depletion have created the need to limit the growth of the world energy consumption and to transition to renewable and eco-friendly energy sources [1,2]. In this context, the production of energy from food waste, along with the production of high-value products, could present a sustainable alternative as well as improve the economic performance of biorefineries [3,4].

The recently revised [5] Renewable Energy Directive 2018/2001 (REDII) [6] provides a common framework for the promotion of

renewable energy in the EU, in context with the European Green Deal [7]. This revision, expected to be adopted by the end of 2022, proposes more ambitious targets in order to achieve climate neutrality in 2050. This includes increasing the renewable energy target to 40 % by 2030. Moreover, REDII requires a minimum of 14 % renewable energy in transport by 2030. In this regard, bioethanol is one of the most well-known renewable fuels, with characteristics such as low boiling point, low toxicity to the environment, high octane number and significant energy content [8]. Moreover, nowadays it is also recognized as a key platform chemical for the production of other fuels including hydrogen, butanol and renewable hydrocarbons, and some chemicals such as acetic

Abbreviations: AH, autohydrolysis; C_{EST} , stoichiometric factor of glucan to glucose conversion; CSR, Cellic CTec2-Substrate Ratio; EtOH, ethanol concentration; $EtOH_{MAX}$, parameter in modified Gompertz equation meaning the potential maximum ethanol concentration; Fru, fructose concentration; Glc, glucose concentration; GGC, Glucan-to-Glucose Conversion; Glc_{MAX} , fitting parameter of Holtzapfle equation measuring the maximum glucose concentration; Gn, glucan content of the pretreated solid; Glc_{pot} , potential glucose concentration; JFc, fermentation of concentrated melon juice; JFc-SSF, sequential fermentation of concentrated melon juice and SSF of autohydrolyzed solid; JFv, fermentation of virgin melon juice; KL, Klason Lignin content; LSR, Liquid-Solid Ratio; MP, Melon Peels; Q_p , Ethanol volumetric productivity; REDII, Renewable Energy Directive 2018/2001; r_m , parameter in modified Gompertz equation meaning the maximum rate of ethanol production; SC, Sugar Content; SHF, Separate Hydrolysis and Fermentation; SSF, Simultaneous Saccharification and Fermentation; SSFc, SSF of autohydrolyzed solid with concentrated melon juice; SSFv, SSF of autohydrolyzed solid with virgin melon juice; $t_{1/2}$, fitting parameter of Holtzapfle equation measuring the reaction time needed to reach a concentration corresponding to 50% of Glc_{MAX} ; t_L , parameter in modified Gompertz equation meaning the phase-lag time; VSR, Viscozyme-Substrate Ratio; WIS, Water-Insoluble Solid; ρ , density.

* Corresponding author at: Universidade de Vigo, Departamento de Enxeñaría Química, Facultade de Ciencias, As Lagoas, 32004 Ourense, Spain.

E-mail address: reme@uvigo.es (R. Yáñez).

<https://doi.org/10.1016/j.fuel.2022.126710>

Received 4 July 2022; Received in revised form 21 October 2022; Accepted 8 November 2022

Available online 18 November 2022

0016-2361/© 2022 The Author(s). Published by Elsevier Ltd. This is an open access article under the CC BY-NC-ND license (<http://creativecommons.org/licenses/by-nc-nd/4.0/>).

acid, ethyl acetate or ethylene [8,9].

The use of agri-food by-products as substrate for bioethanol production is a cheaper and more ethical alternative to the use of food crops such as corn, wheat or rice [10]. However, these by-products are made of complex structures containing mainly cellulose, hemicelluloses, pectin and lignin, and they require a pretreatment step followed by

saccharification and fermentation [11,12]. The saccharification and fermentation steps can be carried out by several strategies, including separate hydrolysis and fermentation (SHF) and simultaneous saccharification and fermentation (SSF), among others [13,14]. SSF has shown increased yields and reduced costs in comparison with SHF, due to the use of a single reactor and a decrease in substrate inhibition associated

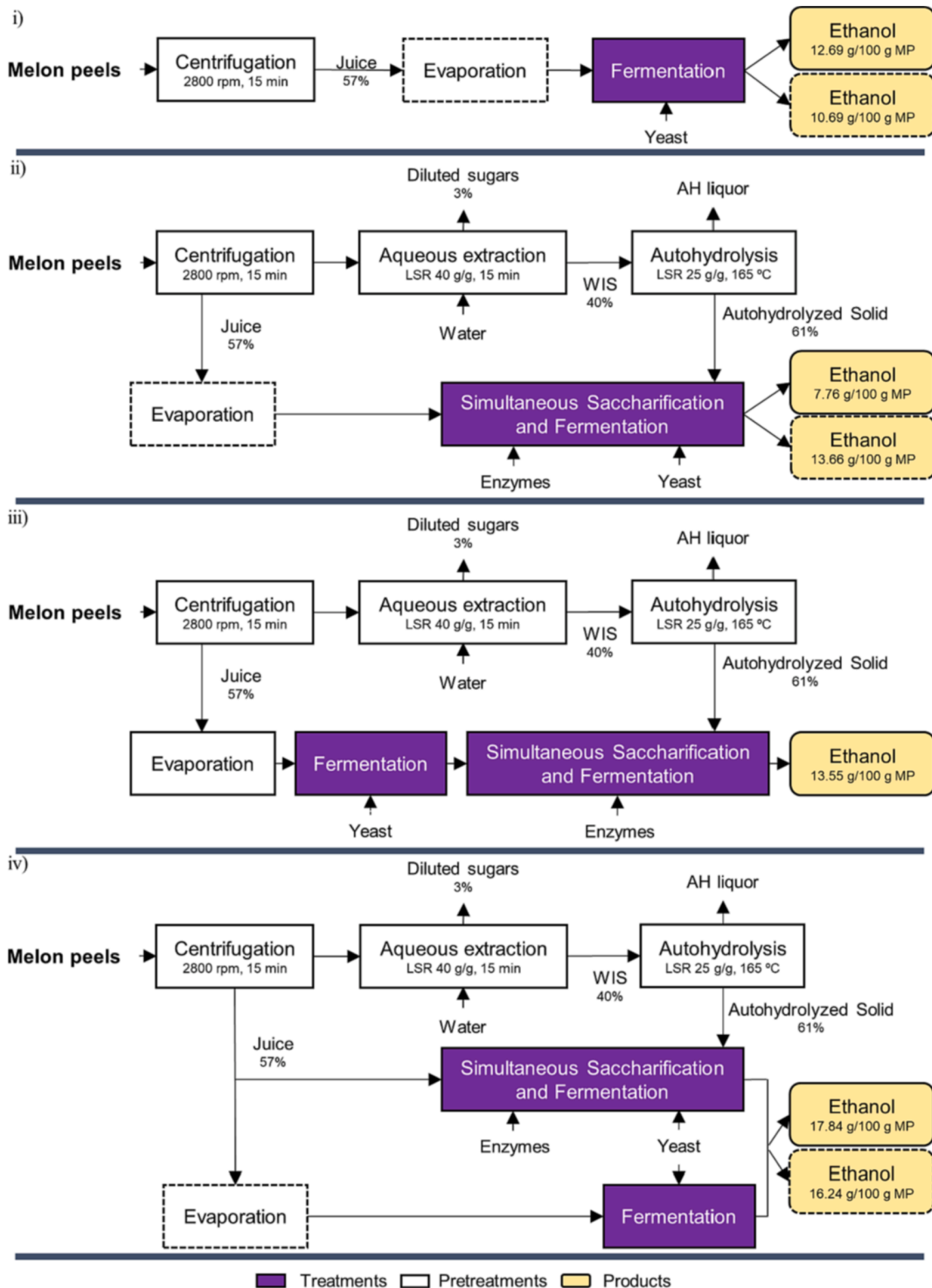


Fig. 1. Flow diagrams of the proposed scenarios in this work. Dotted lines represent alternative treatments and the corresponding results. LSR: liquid–solid ratio; WIS: water-insoluble solid.

with a lower accumulation of sugars [13,15].

In this context, melon peel waste is an abundant agri-food by-product with potential as a raw material for bioethanol production. Melon (*Cucumis melo* L.) is one of the most consumed and produced crops worldwide [16,17]. Its global production fluctuates around 26 million tonnes, with the main producer being China [17], while the main producer in Europe is Spain with 610,980 tonnes per year. The industrial processing of this fruit involves the separation of peels and seeds as by-products, representing 25–44 % and 3–7 % of the weight of the fruit, respectively [18]. Melon by-products are rich in valuable compounds including cellulose, pectin, hemicelluloses, protein and minerals, but are often underutilized [19–21]. Moreover, their content in protein and minerals would be especially beneficial in the formulation of low cost medium for biotechnological processes such as the production of bioethanol.

To date, few authors have evaluated the potential of melon by-products for bioethanol production [22–24]. Salehi et al [22] and Zanivan et al. [23] did not exploit the polysaccharide content of melon peels, while Chaudhary et al. [24] used dilute acid hydrolysis for the saccharification, obtaining 10.30 g/L of ethanol after 6 days. Therefore, the aim of this work was the enhanced production of bioethanol by the valorization of melon peels following several strategies.

2. Materials and methods

Firstly, an experimental design of three variables at three levels (liquid–solid ratio, Cellic® CTec2 loading and Viscozyme loading) was proposed for the optimization of operational conditions in the enzymatic hydrolysis stage. Secondly, with the aim of integrating the valorization of important sugar-containing streams (melon peel juice obtained by an initial centrifugation step, with high contents of glucose, fructose, and protein) and spent solids (obtained by aqueous extraction and autohydrolysis of the centrifuged melon peels) were evaluated as substrates for fermentation. This study comprises the following scenarios (see Fig. 1): i) fermentation of the melon juices (virgin and concentrated); ii) SSF, formulating the culture media with melon juices (virgin and concentrated) and evaluating a fed-batch strategy; iii) sequential fermentation of the concentrated liquors and SSF of the spent solids; and iv) SSF of the spent solids with virgin melon juice and separate fermentation of the remaining juices (virgin and concentrated).

2.1. Raw material

Melon peels (MP) from the “piel de sapo” variety, were kindly supplied by FreshCut, S.L. (Vigo, Pontevedra, Spain). They were cut into small pieces before being frozen at $-18\text{ }^{\circ}\text{C}$ until use.

2.2. Pretreatment

Fig. 1 shows the valorization schemes followed in this work, including the selected pretreatment conditions and production yields.

2.2.1. Aqueous extraction

A centrifugation step at 2800 rpm for 15 min (SV4028, AEG Electrolux) was used to separate a juice fraction rich in fructose, glucose and protein, followed by two aqueous extractions at room temperature for 15 min to eliminate the remaining soluble sugars, using 400 g of wet MP with a liquid solid ratio of 40 g water/g of oven dry MP in a 10 L stirred reactor [25]. The water-insoluble solid (WIS) represented 39.95 % of the MP and was composed mainly of glucan, galacturonan, Klason lignin and protein (24.76, 18.41, 15.70 and 9.70 g/100 g WIS, respectively).

2.2.2. Autohydrolysis

The hydrothermal treatment was carried out as described in a previous work [25]. Wet WIS samples of 80 g were mixed with deionized water (25 g water/g dry WIS) in a 0.6 L stainless steel, pressurized

reactor (model 4842 from Parr Instruments, Moline, IL, USA) and heated up to $165\text{ }^{\circ}\text{C}$, and then cooled immediately. The solid phase was separated by filtration and stored at $-18\text{ }^{\circ}\text{C}$ until use.

2.3. Enzymatic hydrolysis: experimental design

In order to select the saccharification conditions, samples of the autohydrolysis solid were subjected to enzymatic hydrolysis following a Box–Behnken design of three variables at three levels as shown in Table 1. The saccharification experiments were carried out in 100 mL Erlenmeyer flasks at $40\text{ }^{\circ}\text{C}$, pH = 4.85 and 150 rpm using the commercial enzyme preparations Cellic® CTec2 (a blend of cellulases, β -glucosidases and hemicellulases, acquired from Sigma-Aldrich, Steinheim, Germany) and Viscozyme® L (a blend of β -glucanases, pectinases, hemicellulases and xylanases, kindly supplied by Novozymes, Denmark). Samples were withdrawn at timed intervals and then boiled and centrifuged before analysis. The activity of Cellic CTec2 (116 FPU/mL) was determined as filter paper units [26] and the activity of Viscozyme (4348.7 U/mL) as the amount of enzyme able to catalyze the formation of 1 μmol of galacturonic acid per min at $37\text{ }^{\circ}\text{C}$ and pH = 5 from polygalacturonic acid 0.5 % [27].

The glucan-to-glucose conversion (GGC) was determined following equation (1) and fitted to the Holtzapfle equation [28] (equation (3)).

$$\text{GGC} (\%) = \frac{(\text{Glc}_t - \text{Glc}_0)}{\text{Glc}_{\text{pot}}} \quad (1)$$

$$\text{Glc}_{\text{pot}} (\text{g/L}) = \frac{\text{Gn}/\text{C}_{\text{Est}} \cdot \rho}{\text{LSR} + 1 - \text{KL}} \quad (2)$$

$$\text{Glc}_t (\text{g/L}) = \text{Glc}_{\text{MAX}} \frac{t}{t + t_{1/2}} \quad (3)$$

where Glc_t and Glc_0 are glucose concentrations at times t and 0, Glc_{pot} is the potential glucose concentration, Gn is the glucan content of the pretreated solid, C_{Est} is the stoichiometric factor, ρ is the density of the medium, LSR is the liquid to solid ratio, KL is the Klason lignin content of the pretreated solid and Glc_{MAX} and $t_{1/2}$ are fitting parameters measuring the maximum glucose concentration at an infinite time and the reaction time needed to reach a concentration corresponding to 50 % of Glc_{MAX} , respectively.

Table 1

Experimental design for the enzymatic hydrolysis in terms of the dimensional variables LSR (liquid–solid ratio), CSR (Cellic CTec2-substrate ratio) and VSR (Viscozyme-substrate ratio) and dimensionless variables x_1 – x_3 .

Experiment number	Dimensional, independent variables			Dimensionless, independent variables		
	LSR (g/g)	CSR (FPU/g)	VSR (U/g)	x_1	x_2	x_3
1	10	5	25	-1	-1	0
2	10	17.5	10	-1	0	-1
3	10	17.5	40	-1	0	1
4	10	30	25	-1	1	0
5	17.5	5	10	0	-1	-1
6	17.5	5	40	0	-1	1
7	17.5	17.5	25	0	0	0
8	17.5	17.5	25	0	0	0
9	17.5	17.5	25	0	0	0
10	17.5	30	10	0	1	-1
11	17.5	30	40	0	1	1
12	25	5	25	1	-1	0
13	25	17.5	10	1	0	-1
14	25	17.5	40	1	0	1
15	25	30	25	1	1	0

2.4. Microorganism and inoculum preparation

Ethanol Red®, a commercial *Saccharomyces cerevisiae* strain, was grown at 30 °C and 200 rpm for 12–14 h in a medium containing 20 g peptone/L, 10 g yeast extract/L and 20 g glucose/L. This process was repeated once at the same conditions, and the grown yeast was employed as inoculum in fermentation experiments.

2.5. Fermentation

Several fermentation experiments were carried out following the scenarios shown in Fig. 1.

Scenarios i, iii and iv include the fermentation of melon peel juice samples from the first centrifugation step (virgin or concentrated). The concentration of the juice was performed by rotary evaporation (R-210, Buchi, Switzerland), whereas the fermentation was carried out at 40 °C and 120 rpm for 48 h (6 h for scenario iii) in an orbital shaker with 1.5 g/L of inoculum (dry basis), with and without nutrients (20 g peptone/L and 10 g yeast extract/L).

The simultaneous saccharification and fermentation (SSF) of the autohydrolysis solid was carried out in scenarios ii, iii and iv. The saccharification conditions for these experiments were selected previously by experimental design of the enzymatic hydrolysis (LSR of 10 g/g, CSR of 17.5 FPU/g and VSR of 25 and 40 U/g). The use of external nutrients was studied using 20 g peptone/L and 10 g yeast extract/L. Melon peel juice from the first centrifugation step (virgin and concentrated) was used for the formulation of the medium instead of water.

A fed-batch strategy was assessed at the same conditions, starting with a LSR of 10 g/g and adding another 50 % of the feed, with the corresponding amount of enzymes, after 12 h of fermentation.

In scenarios ii and iii, the spent solid fraction was added at initial time and after 6 h of fermentation, respectively. In these cases, in order to propose a zero waste global process, the LSR was increased to 11.4 g/g, maintaining all the other previous experimental conditions.

Samples were withdrawn at timed intervals, and they were centrifuged before analysis. Ethanol yield and volumetric productivity (Q_p) were calculated following equations (4) and (5), and ethanol concentrations were fitted to the modified Gompertz model [29] (eq. (6)):

$$\text{Ethanol yield (\%)} = \frac{(\text{EtOH}_t - \text{EtOH}_0)}{0.51 \cdot \text{SC}} \quad (4)$$

$$Q_p \text{ (g/L} \cdot \text{h)} = \frac{\text{EtOH}_t}{t} \quad (5)$$

$$\text{EtOH}_t \text{ (g/L)} = \text{EtOH}_{\text{MAX}} \cdot \exp \left[- \exp \left[\frac{r_m \cdot \exp(1)}{\text{EtOH}_{\text{MAX}}} (t_L - t) + 1 \right] \right] \quad (6)$$

where EtOH_t and EtOH_0 are ethanol concentrations at times t and 0, 0.51 is the stoichiometric factor for glucose to ethanol conversion, SC is the total sugar content in g/L, including hexoses in the juice, in the enzyme preparations and in the solid (as monomers), EtOH_{MAX} is the potential maximum ethanol concentration (g/L), r_m is the maximum rate of ethanol production (g/Lh) and t_L is the phase-lag time (h).

2.6. Analytical methods

2.6.1. Analysis of the solids

Samples of WIS and autohydrolysis solids were dried at 60 °C until constant weight and subjected to moisture (TAPPI T-264-om-88 method) and ash (T-244-om-93 method) determination. Minerals were determined by atomic absorption spectrometry (Varian Spectra AA 220/FS), for which microwave assisted acid digestion was carried out with 5 mL of HNO_3 65 % (w/w), 1 mL of H_2O_2 30 % (w/v) and 0.5 mL of HF 40 % (w/w). Protein content was calculated from the nitrogen content (assuming 6.25 g protein/g nitrogen), determined with an elemental analyzer (Thermo Finnigan EA 1112). Finally, conventional quantitative

acid hydrolysis with 72 % H_2SO_4 (TAPPI T13 m method) was used to determine the content of hemicelluloses, glucan and Klason lignin. The oven-dried solid residue from hydrolysis was considered as Klason lignin (TAPPI T13 m assay), while the liquid phase was analyzed by HPLC using an Agilent 1260 equipped with a refractive index (RI) detector. Citric acid, rhamnose, arabinose and acetic acid were separated using an Aminex HPX-87H column (BioRad, Life Science Group, Hercules, CA), operating with 3 mM H_2SO_4 as the mobile phase, at a flow rate of 0.6 mL/min at 50 °C; whereas glucose, sucrose, xylose, galactose, mannose and fructose were separated with a CARBOsep CHO-682 Pb column (Transgenomic, Glasgow, UK) operating with deionized water as the mobile phase, at 0.4 mL/min and 80 °C. An aliquot of the liquid phase was also subjected to uronic acid determination by spectrophotometry, with galacturonic acid as standard [30].

2.6.2. Chemical characterization of liquors

Samples from the enzymatic hydrolysis and fermentation experiments were filtered through 0.45 μm membranes and analyzed for glucose, fructose and ethanol by HPLC using an Agilent 1260 equipped with a refractive index (RI) detector and an Aminex HPX-87H column (BioRad, Life Science Group, Hercules, CA), operating with 3 mM H_2SO_4 as the mobile phase, at a flow rate of 0.6 mL/min at 50 °C.

2.7. Data analysis

All the data were analyzed using the commercial software Microsoft Excel (Microsoft, USA). The regression coefficients and statistical parameters (ANOVA test) were also obtained using Microsoft Excel.

3. Results and discussion

3.1. Pretreatment of the raw material

The schemes followed in this work are shown in Fig. 1. The pretreatment steps included an initial centrifugation of melon peels for the recovery of a juice rich in fermentable sugars, and (in schemes ii, iii and iv) an aqueous extraction of the centrifuged solid to eliminate the remaining soluble sugars. The water insoluble solid (WIS) from schemes ii, iii and iv was then subjected to non-isothermal autohydrolysis at 165 °C, resulting in a liquid fraction containing pectic oligosaccharides and phenolic compounds [25] and a solid fraction enriched in cellulose and lignin.

3.2. Chemical composition

Table 2 details the chemical composition of the melon peel juice (57 % of the raw material) and of the autohydrolyzed solid (24 % of the raw material). Fermentable sugars (glucose, fructose and sucrose) accounted for 58.42 % of the non-volatile content of the juice, which also had high contents of ash and protein. Regarding the autohydrolysis solid, it had a high moisture content (61.68 %) and its main components were glucan and lignin with percentages of 36.69 and 25.50 %, respectively, and recoveries of 98.21 and 99.53 % from their respective contents in the WIS. These results can be favorably compared with the glucan content of hydrothermally treated pomegranate peels (25–26 %) [31] and cocoa pod husks (21.22 %), which also contained a higher lignin content (41.60 %) [32]. The protein content of the solid should also be noted due to its nutritional value for the fermentation medium. In this line, the mineral content of both solid and juice could also have a positive effect in bioethanol production [33,34]. Potassium, sodium, magnesium and calcium were found in high amounts in the juice, while the solid showed higher calcium and iron contents.

3.3. Assessment of the enzymatic hydrolysis

The evaluation of the enzymatic hydrolysis conditions was proposed

Table 2
Composition of the melon peel juice and the autohydrolyzed solid.

a) Composition of the two fractions		
Component	Content	
Juice (g/100 g dry weight)		
Citric Acid	2.46 ± 0.01	
Glucose	23.50 ± 0.14	
Fructose	25.46 ± 0.15	
Sucrose	9.46 ± 0.06	
Protein	12.87 ± 0.14	
Ash	17.52 ± 0.15	
Autohydrolyzed solid (g/100 g dry weight)		
Glucan	39.69 ± 0.36	
Galacturonan	7.91 ± 0.21	
Xylan	2.00 ± 0.07	
Galactan	2.35 ± 0.26	
Mannan	2.07 ± 0.23	
Arabinosyl Substituents	0.79 ± 0.04	
Acetyl Groups	1.05 ± 0.04	
Klason Lignin	25.50 ± 1.84	
Protein	9.03 ± 0.52	
Ash	2.56 ± 0.09	
b) Mineral content (mg/100 g dry weight)		
Component	Autohydrolyzed solid	Juice
Magnesium	138.95 ± 7.22	690.44 ± 10.04
Calcium	854.24 ± 52.78	630.56 ± 8.75
Potassium	30.44 ± 2.00	6,445.45 ± 63.50
Sodium	9.30 ± 3.86	858.40 ± 6.79
Zinc	3.99 ± 0.24	5.39 ± 0.08
Copper	1.10 ± 0.10	–
Iron	11.97 ± 0.35	2.12 ± 0.02
Manganese	2.01 ± 0.09	1.60 ± 0.07

as the first step to study the bioethanol production from autohydrolyzed melon peels. The Cellic® CTec2 enzyme blend was selected due to its cellulase and β-glucosidase activities. However, preliminary experiments carried out showed a really high viscosity at low LSR which hindered the hydrolysis completely. In view of this, Viscozyme® L (an enzyme blend including pectinase, β-glucanase, hemicellulose and xylanase activity) was added in order to reduce the viscosity of the medium as previously reported in the literature [35,36]. The positive results obtained proved the need of this enzyme, which was included as an independent variable in the next experiments.

In order to determine the most favorable conditions for the enzymatic saccharification, an experimental design of three variables at three levels was proposed. The studied variables were liquid–solid ratio (LSR, 10–25 g/g), Cellic CTec2 to substrate ratio (CSR, 5–30 FPU/g) and Viscozyme to substrate ratio (VSR, 10–40 U/g).

Table 3
Holtzapfle parameters obtained in experiments 1–15.

Expt	Glc _{MAX} (g/L)	t _{1/2} (h)	R ²
1	36.30	9.94	0.998
2	40.23	4.84	0.998
3	42.11	4.98	0.992
4	38.52	3.15	0.962
5	23.31	6.12	0.996
6	25.27	6.42	0.964
7	23.30	1.83	0.977
8	23.06	2.03	0.991
9	24.11	2.69	0.989
10	21.04	0.75	0.971
11	23.27	1.36	0.996
12	15.77	5.90	0.992
13	16.11	2.30	0.992
14	19.79	6.00	0.995
15	15.34	0.96	0.968

3.3.1. Experimental data of enzymatic kinetics

Table 3 shows the results for the Holtzapfle equation parameters (Glc_{MAX} and t_{1/2}) and the correlation coefficient (R²) for each of the experiments presented in Table 1.

As can be seen in Table 3, the experimental data was well fitted by the empirical equation proposed (R² between 0.962 and 0.998). The theoretical maximum glucose concentrations (Glc_{MAX}) reached over 90 % of the glucose potential (Glc_{Pot}) in almost every experiment (with the exceptions being experiments 1, 10 and 15), demonstrating the high enzymatic susceptibility of the autohydrolyzed solid. Moreover, all the experiments showed fast saccharifications with glucose concentrations of 85–97 % of Glc_{MAX} at 32 h, except for experiment 1, which also had the highest t_{1/2} value of 9.94 h. The fastest saccharifications were found in experiments 10, 11 and 15 (t_{1/2} of 0.75–1.36 h), performed at the highest CSR. The same cannot be said for experiment 4, also using the highest CSR but the lowest LSR. However, exp. 4 was still faster than other experiments with the same LSR (expts. 1–4).

3.3.2. Optimization of enzymatic hydrolysis of autohydrolyzed solid fraction: Application of the response surface methodology

Response surface methodology was used for the interpretation of the effect of the operating conditions on the dependent variables. This method is useful to determine the interactions between independent and dependent variables with a reduced number of experiments [37,38]. For this purpose, the parameters Glc_{MAX}, t_{1/2} and GGC_{32h} (glucan to glucose conversion at 32 h) were fitted to empirical models following equation (7).

$$y_j = b_{0j} + \sum_{i=1}^3 b_{ij}x_i + \sum_{i=1}^3 \sum_{k \geq i}^3 b_{ijk}x_i x_k \quad (7)$$

Where y_j is the dependent variable (Glc_{MAX}, t_{1/2}, and GGC_{32h}), x_i or x_k are the normalized independent variables (LSR, CSR and VSR) and b_{0j}–b_{ijk} are the regression coefficients calculated by multiple regression with the least-squares method. The regression coefficients and the ANOVA data are detailed in Table 4. All the correlations were significant and presented good fits with R² values over 0.9.

According to the coefficients shown in Table 4, the negative linear term of LSR was the most influential factor for Glc_{MAX}, followed by the positive quadratic term of the same variable and the negative quadratic term of the CSR. Fig. 2a, represents the calculated dependence of Glc_{MAX} on LSR and CSR at fixed VSR values (10, 25 and 40 U/g). Glc_{MAX} reached the highest values at lower LSR and intermediate CSR. Meanwhile, VSR had a positive effect on the theoretical maximum glucose concentrations, although it was the least influential variable. The maximum Glc_{MAX} predicted by the model was 41.63 g/L, reached at CSR 19.06

Table 4

Regression coefficients and statistical parameters measuring the correlation and significance of models (based on ANOVA test) for the selected dependent variables.

Parameter	Glc _{MAX} (g/L)	t _{1/2} (h)	GGC _{32h} (%)
Intercept	23.491*	2.183**	91.773*
x ₁ (LSR)	−11.269*	−0.970**	3.213**
x ₂ (CSR)	−0.311	−2.769*	3.577**
x ₃ (VSR)	1.220**	0.593	4.187**
x ₁ x ₂	−0.663	0.462	−2.338
x ₁ x ₃	0.452	0.890	1.815
x ₂ x ₃	0.066	0.080	−0.472
x ₁ ²	4.664*	1.835**	−4.447***
x ₂ ²	−1.673**	0.969	−8.230*
x ₃ ²	1.406***	0.512	3.928***
Significance	99.996	99.215	97.561
SD	1.126	0.946	3.517
R ²	0.994	0.953	0.924
Adj-R ²	0.984	0.869	0.787

*, significant coefficients at the 99 % confidence level; **, significant coefficients at the 95 % confidence level; ***, significant coefficients at the 90 % confidence level.

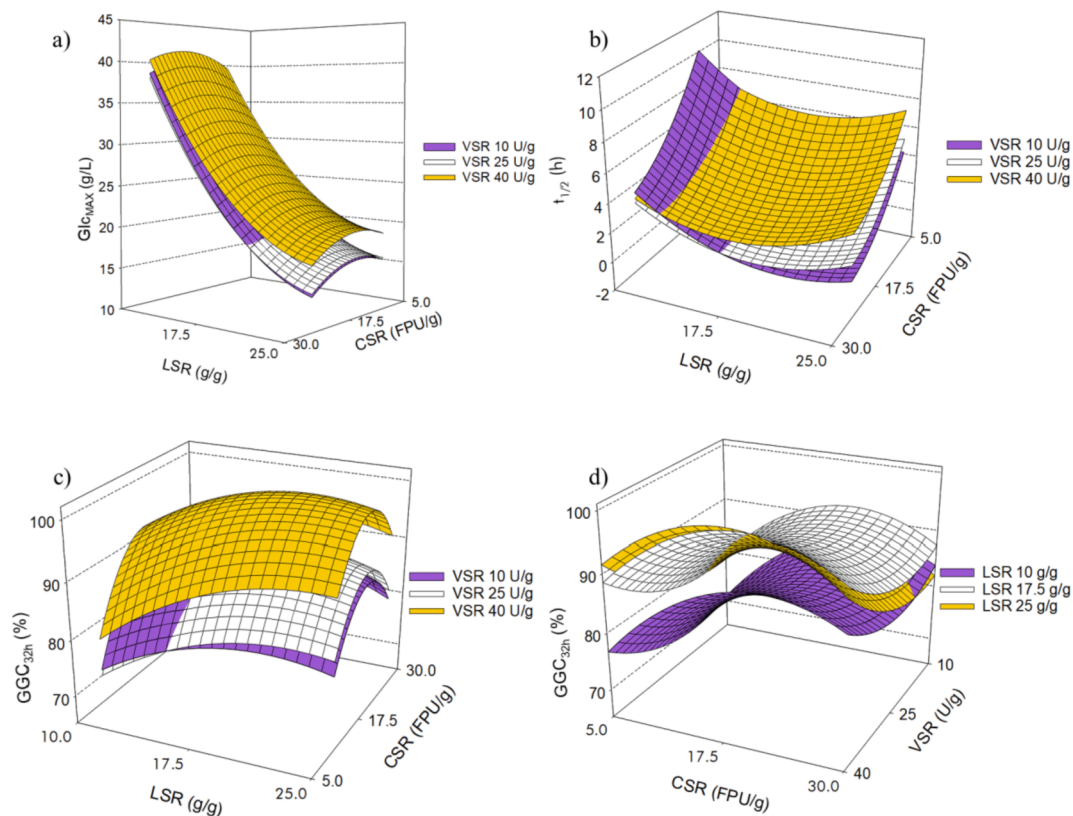


Fig. 2. Response surfaces: a) Glc_{MAX} at VSR of 10, 25 and 40 U/g; b) $t_{1/2}$ at VSR of 10, 25 and 40 U/g; c) GGC_{32h} at VSR of 10, 25 and 40 U/g and d) at LSR of 10, 17.5 and 25 g/g.

FPU/g, LSR 10 g/g and VSR 40 U/g.

The dependence of $t_{1/2}$ on LSR and CSR at VSR of 10, 25 and 40 U/g is shown in Fig. 2b. As can be inferred by the model coefficients in Table 4, although both variables are significant, CSR had a higher effect on this parameter than LSR. Higher CSRs result in lower $t_{1/2}$, denoting a positive effect on the saccharification rate. The same behavior has been found in the literature for other raw materials, such as apple pomace and *Eucalyptus globulus* wood [39,40]. Regarding LSR, its quadratic term was more influential than the linear one and its positive value indicates a minimum, which can be seen in Fig. 2b at around 17–23 g/g.

In order to assess the effect of the dependent variables on glucan-to-glucose conversion (GGC), the values at 32 h were fitted to the model. At this time, saccharifications were almost complete with GGC ranging from 67.08 to 100.00 %, corresponding to experiments 1 and 14. As can be seen by the coefficients in Table 4, all three lineal terms had a significant and positive effect on GGC_{32h} , while the quadratic term of CSR was the most influential variable.

Fig. 2c and d represent the calculated dependence of GGC_{32h} on LSR and CSR at VSR of 10, 25 and 40 U/g, and on CSR and VSR at LSR of 10, 17.5 and 25 g/g, respectively. As can be seen in Fig. 2c, GGC_{32h} response surfaces reached maximum values at intermediate CSR (18–23 FPU/g) and intermediate to high LSR (17–25 g/g), decreasing slightly afterwards as reflected by the negative sign of their quadratic terms, being this effect less pronounced for the LSR. Concerning VSR, the highest values for the GGC_{32h} (76.74–100 %) were predicted for VSR of 40 U/g. In general terms, from Fig. 2d it should be noted the positive effect of intermediate to high LSR (range 17.5–25 g/g) on the GGC_{32h} .

Taking into account the response surfaces assessment, the selected conditions to continue the study were LSR 10 g/g, CSR 17.5 FPU/g and VSR 40 U/g. The lowest LSR was selected in order to improve the economic viability of the process, while an intermediate CSR allowed obtaining high yields and concentrations at fast rates. Regarding VSR, the highest loading was selected due to the notable decrease in the

viscosity of the medium, as well as its positive effect on GGC and Glc_{MAX} . At these conditions, the experimental results showed that 35.15 g/L of glucose were released after 24 h of saccharification, representing a conversion of 85.66 %. The selected models at the same conditions predicted a Glc_{MAX} of 41.60 g/L, $t_{1/2}$ of 5.20 h and a GGC_{32h} of 90.41 %, close to the experimental one of 90.63 %.

The conversion yields obtained at the selected conditions were higher than those obtained in a previous work (79.83 % at 24 h and 87.65 % at 48 h) using melon by-products autohydrolyzed at a lower temperature (140 vs 165 °C), with a LSR of 12 g/g, 12 FPU/g and 50 U Viscozyme/g [21]. This comparison suggests that a higher severity can improve the enzymatic susceptibility as indicated in the literature [14,41]. An explanation for this would be a further removal of hemicelluloses and pectin, which would limit the accessibility for the enzymes, and of the phenolic compounds, which are known inhibitors [14,31,42].

Furthermore, similar conversion yields have been found in the literature using pectin rich raw materials pretreated by autohydrolysis. Talekar et al. [31] achieved a conversion of 95 % after 36 h for pomegranate peels when using a solid loading of 12 % (LSR of 7.3 g/g) and a cellulase loading of 30 U/g of glucan. On the other hand, lower yields (69 %) were also found for cocoa pod husk, using 5 % solid loading (LSR of 19 g/g) and 15–20 FPU/g of substrate [32].

3.4. Strategies evaluated for bioethanol production

As stated in methods section, the fermentation experiments were carried out using a commercial *Saccharomyces cerevisiae* strain (Ethanol Red®).

3.4.1. Fermentation of melon peel juice

The fermentation of melon peel juice, a process stream with interesting sugar and nutrients contents (including protein and minerals, see

Table 2), was one of the proposed steps in every-one of the scenarios shown in Fig. 1. Therefore, the first fermentation experiments in this study were meant to evaluate the fermentability of this stream. For that, a batch fermentation with and without nutrients (20 g peptone/L and 10 g yeast extract/L) was performed in the experimental conditions previously stated in materials and methods section.

Since no differences were found with the addition of nutrients, the presented results (Fig. 3a) are the ones without external nutrients. The production of ethanol was fitted to the modified Gompertz model, which can provide a prediction of the maximum production, the maximum productivity and the phase-lag time [29,43]. The results were well fitted to the model ($R^2 = 1.000$), with a similar maximum concentration as the experimental one (13.06 vs 13.10 g/L).

3.4.2. Simultaneous saccharification and fermentation experiments performed with melon peel juice

A set of four SSF experiments was performed in order to evaluate the effects of the saccharification stage, the viscosity of the medium and the addition of nutrients on the ethanol production. For this, high to intermediate levels of Viscozyme were tested (VSR of 40 and 25 U/g), with

and without external nutrients (20 g peptone/L and 10 g yeast extract/L). Moreover, to integrate the melon peel juice in the SSF stage, this stream was used in all experiments for the formulation of the medium instead of water, to provide additional sugars (27.42 g/L) at the beginning of the fermentation, as well as nutrients (see scenarios ii and iv in Fig. 1). The temperature was maintained at 40 °C, whereas the LSR and the CSR were fixed in 10 g/g and 17.5 FPU/g, respectively, conditions previously selected by the enzymatic hydrolysis.

Since no important differences were detected among the four experiences, the one without nutrients using VSR = 40 U/g was selected as a representative example. The time course of sugars (glucose and fructose) and ethanol is shown in Fig. 3b, as well as the calculated curve for ethanol production using the modified Gompertz model.

In all experiments, the consumption of sugars was fast, especially for glucose, with concentrations between 0.43 and 0.81 g/L after 6 h, time at which the highest volumetric productivities were found: 3.87–4.29 g/Lh. These values can be positively compared with Zanivan and co-workers' study, who reached a Q_p of 2.50 g/Lh at 9 h of operation using mixed fruit waste (including melon waste) without nutrients and without a saccharification pretreatment [23]. Moreover, Chaudhary

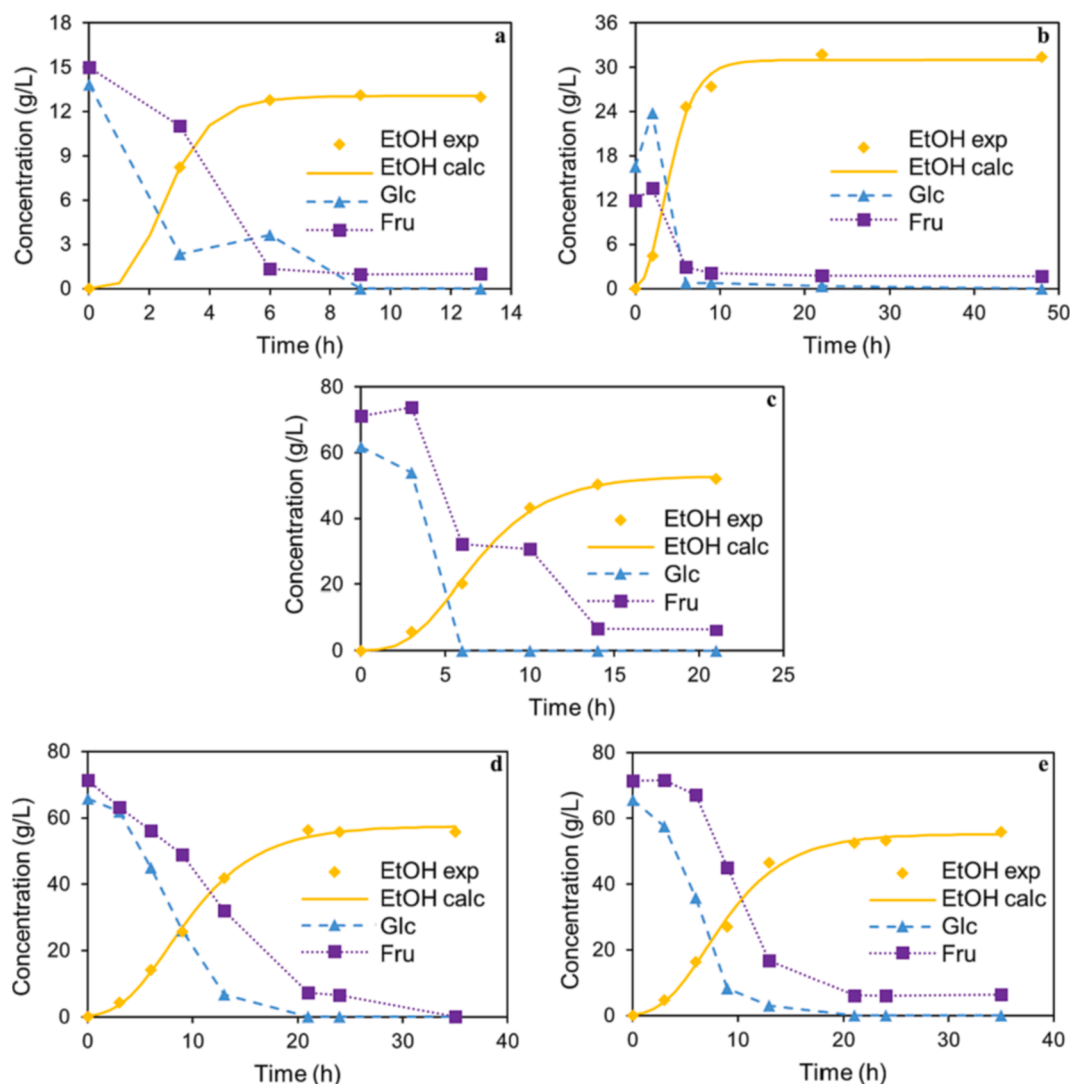


Fig. 3. Glucose, fructose and ethanol time courses of a) fermentation of virgin melon peel juice (JFv), b) SSF of the autohydrolyzed solid at LSR 10 g/g, CSR 17.5 FPU/g and VSR 40 U/g with virgin melon juice (SSFv), c) fermentation of concentrated melon juice (JFc), d) SSF of the autohydrolyzed solid at LSR 11.4 g/g, CSR 17.5 FPU/g and VSR 40 U/g with concentrated melon juice (SSFc), and e) fermentation of the concentrated melon juice with sequential SSF of the autohydrolyzed solid at LSR 11.4 g/g, CSR 17.5 FPU/g and VSR 40 U/g (JFc-SSF). All the presented fermentations were carried out without external nutrients. Ethanol solid line represents the predicted values by modified Gompertz model. EtOH: ethanol; Glc: glucose; Fru: fructose.

et al. [24] achieved an even lower productivity (10.30 g ethanol/L after 6 days) from melon peels using a dilute acid saccharification step followed by fermentation with nutrient addition (yeast extract, $(\text{NH}_4)_2\text{SO}_4$, KH_2PO_4 , $\text{MgSO}_4 \cdot 7\text{H}_2\text{O}$, CaCl_2 , ZnCl_2).

After 6 h, ethanol concentrations kept increasing until reaching a maximum at 22 h, with values between 29.96 and 31.70 g/L. These concentrations were similar to the potential maximum ethanol concentrations obtained by the modified Gompertz model (28.39–30.99 g/L), which presented a good fit for the four experiments ($R^2 > 0.99$). The r_m and t_L values were 5.37–7.31 g/Lh and 1.03–1.30 h, respectively. Lower rates were found in the literature for corn cobs (1.25 g/Lh) and potato peels (1.51 g/Lh) [44,45], while the lag time was shorter for corn cobs and longer for potato peels. Meanwhile, similar r_m and t_L values were reported by Dodić et al. [46] for sugar beet raw juice: 4.39 g/Lh and 1.04 h, respectively.

Regarding bioethanol yields, favorable values were also obtained at 22 h, in the range 71.12–75.26 %. A similar maximum yield of 74 % was reported in another study following a similar approach with sweet sorghum bagasse [47]. Both juice and autohydrolyzed solid of sweet sorghum bagasse were subjected to SSF, achieving the maximum ethanol concentration after a long fermentation time of 168 h, whereas after 24 h the yield was only around 60 %.

When compared to other pectin-rich raw materials, the yields in this work were lower than for steam pretreated sugar beet pulp and autohydrolyzed pomegranate peel [31,48,49]. However, ethanol concentrations and productivities were generally higher due to the integration of the juice stream into the process. In the same line, Patsalou et al. [50] recycled the liquid phase of the acid hydrolysis pretreatment of citrus peels into the enzymatic hydrolysis stage of the solid phase, increasing the ethanol concentration from 9.2 to 30.7 g/L.

The minor differences found between the four experiments proved that the addition of external nutrients was not necessary, which is in agreement with the previously mentioned study by Rohowsky et al. [47] with a similar approach.

3.4.3. Assessment of a fed-batch approach

In order to increase the final ethanol concentration, the following fed-batch strategy was proposed: 1) beginning with LSR of 10 g/g, CSR of 17.5 FPU/g and VSR of 40 U/g; and 2) adding a second solid loading at 12 h, with half the amount of solid and the corresponding amount of enzymes, reaching a final LSR of 7.3 g/g. In this context, it should be noted that the fed-batch mode can be used to alleviate the high viscosities of the medium associated to high solid loadings and to lower yields [51].

Although the maximum concentration in this work was raised a 17 %, from 31.70 to 36.96 g/L operating in fed-batch mode, the fermentation media did not tolerate additional solid charges and therefore other approaches were further proposed to improve the final ethanol contents.

3.4.4. Fermentation of concentrated melon juice

The concentration of the melon peel juice by rotatory evaporation was proposed as another approach to increase the ethanol concentration. This way, the concentrations of sugars were 67.33 g glucose/L, 70.43 g fructose/L and 12.02 g sucrose/L. The fermentation of the concentrated juice (a step considered in scenarios i and iv from Fig. 1) was evaluated with and without nutrients, obtaining similar results in both cases.

The time course of glucose concentration was similar to the SSF (see Fig. 3c for the fermentation without nutrients), obtaining a complete depletion after 6 h, whereas the consumption of fructose was slower. Therefore, the maximum productivity of 4.33 g/Lh was found at a later time of 10 h. The maximum experimental ethanol concentration (51.95 g/L) was achieved after 21 h, corresponding to an ethanol yield of 68 % (lower than the ones reached with the virgin juice). This fermentation presented a good fit with the modified Gompertz equation, with an R^2 of

0.998 and the parameters $\text{EtOH}_{\text{MAX}} = 52.92$ g/L, $r_m = 6.71$ g/Lh and $t_L = 2.79$ h.

3.4.5. Simultaneous saccharification and fermentation with concentrated juice

In order to improve the final ethanol concentrations in a one-vessel process, a new SSF experiment (denoted as SSFc) adding concentrated juice to the media was carried out (see scenario ii in Fig. 1). Moreover, another two steps, one-vessel strategy (JFc-SSF) was evaluated to assess the effect of the concentrated juice on the saccharification: fermentation of the concentrated juice for 6 h (when most of the sugars were already consumed), followed by the simultaneous saccharification and fermentation of the autohydrolyzed solid (scenario iii in Fig. 1). In both fermentations, the LSR was adjusted to 11.4 g/L in order to use the total amount of melon peel juice and propose a zero waste global process.

The time course of these two experiments can be seen in Fig. 3d and e. There were no notable differences between the results of the two SSFs, but the higher viscosity of the medium in SSFc was visually evident. The maximum ethanol concentrations (56.24 and 55.81 g/L) were achieved after 21 and 35 h, for SSFc and JFc-SSF, respectively, whereas the maximum productivities were achieved at the same time for both SSFs (3.22 and 3.57 g/Lh for SSFc and JFc-SSF, at 13 h). This was slower than the fermentation with virgin juice, in which the maximum productivity was found after 6 h. Moreover, the yields corresponding to the maximum concentrations were 61.22 and 60.75 %, lower than the one achieved in the SSF using virgin juice (75.26 %), which is in agreement with the results for the fermentation of concentrated vs virgin juice.

3.5. Comparison of the proposed scenarios

The main results of the fermentation experiments, including the parameters of the modified Gompertz model, are collected in Table 5, as well as the total ethanol production of the four scenarios proposed in Fig. 1.

In general, the fermentations using virgin melon juice achieved higher yields at faster rates. This derives into higher bioethanol production in regards to the amount of raw material used. For instance, the juice fermentation (scenario i) produced 12.69 g of bioethanol/100 g MP (dry weight) when using the virgin juice, but only 10.69 g/100 g MP when using the concentrated one. On the other hand, both cases compare favorably with the amount of bioethanol produced from the soluble sugars in melon waste by Salehi et al. [22], 6.05 g/100 g MP.

Regarding the SSF schemes (scenario ii), the use of concentrated juice increased the bioethanol production from 7.76 to 13.66 g/100 g MP, whereas the use of a pre-fermentation stage did not improve the production further (scenario iii), and the use of a fed-batch approach lowered the production to 6.10 g/100 g MP. However, in the case of the SSF using virgin juice (SSFv), there is leftover juice that could still be fermented either in its virgin state or concentrated. This is the case of scenario iv, where the bioethanol production of 7.76 g/100 g MP can be increased to a total of 17.84 or 16.24 g/100 g MP (for virgin and concentrated, respectively) when the remaining juice is fermented separately.

Even though the fermentations with virgin juice achieved higher productions, ethanol concentrations were always under 40 g/L, which is the benchmark for a techno-economically viable distillation [52]. Therefore, the use of concentrated juice should be evaluated taking into account the cost of both the evaporation and the distillation.

The ethanol concentrations obtained in every scenario evaluated were higher than those achieved by Chaudhary et al. [24] (10.30 g ethanol/L). In this study, melon peels were pretreated with dilute sulfuric acid and the liquid phase was subjected to neutralization and detoxification stages before performing the fermentation with the addition of external nutrients.

In this work, several strategies for bioethanol production were proposed by evaluating the final ethanol concentrations and productions.

Table 5

Parameters calculated by modified Gompertz equation and experimental results obtained for the following experiences: JFv, JFc, SSFv, SSFc and JFc-SSF; and bioethanol production for each of the proposed scenarios.

Exp.	Gompertz model parameters				Experimental results		
	EtOH _{MAX} (g/L)	r _m (g/Lh)	t _L (h)	R ²	EtOH _{MAX} (g/L)	Q _{pMAX} (g/Lh)	Yield _{MAX} (%)
JFv	13.06	4.92	1.27	1.000	13.10	2.74	83.75
JFc	52.92	6.71	2.79	0.998	51.95	4.33	68.00
SSFv	30.99	5.60	1.26	0.995	31.70	4.11	75.26
SSFc	57.49	4.55	3.06	0.998	56.24	3.22	61.22
JFc-SSF	55.21	4.87	2.82	0.995	55.81	3.57	60.75

Scenario	Description	g EtOH/100 g MP
i)	Fermentation of virgin melon juice (JFv)	12.69
	Fermentation of concentrated melon juice (JFc)	10.69
ii)	SSF of autohydrolysis solid with virgin melon juice (SSFv)	7.76
	SSF of autohydrolysis solid with concentrated melon juice (SSFc)	13.66
iii)	Sequential fermentation of concentrated melon juice and SSF of autohydrolysis solid (JFc-SSF)	13.55
iv)	SSF of autohydrolysis solid with virgin melon juice (SSFv) and separate fermentation of remaining virgin melon juice (JFv)	17.84
	SSF of autohydrolysis solid with virgin melon juice (SSFv) and separate fermentation of remaining concentrated melon juice (JFc)	16.24

Future studies should focus on the techno-economic and environmental viability of the different scenarios, including the valorization of the autohydrolysis liquors.

4. Conclusions

Melon peels were subjected to different strategies for bioethanol production using both a juice fraction obtained by centrifugation and a solid fraction obtained by autohydrolysis. Firstly, the conditions for the enzymatic hydrolysis of the solid were selected by response surface assessment, achieving a glucose concentration of 35.15 g/L after 24 h. Afterwards, the fermentability of the juice was assessed, as well as the SSF with co-fermentation of the juice. The maximum bioethanol production was obtained by SSF and separate fermentation of the remaining virgin juice (17.84 g/100 MP), while the highest concentration was achieved by SSF with concentrated juice (56.24 g/L).

CRedit authorship contribution statement

Xiana Rico: Conceptualization, Methodology, Software, Formal analysis, Investigation, Writing – original draft, Visualization. **Remedios Yáñez:** Conceptualization, Methodology, Validation, Formal analysis, Resources, Writing – review & editing, Visualization, Supervision, Project administration, Funding acquisition. **Beatriz Gullón:** Conceptualization, Methodology, Software, Validation, Formal analysis, Investigation, Resources, Writing – review & editing, Visualization, Supervision, Project administration, Funding acquisition.

Declaration of Competing Interest

The authors declare that they have no known competing financial interests or personal relationships that could have appeared to influence the work reported in this paper.

Data availability

Data will be made available on request.

Acknowledgements

This work was supported by the “Xunta de Galicia” (GRC ED431C 2018/47, Centro Singular de Investigación Biomédica “CINBIO” and Project ED431F 2020/03, partially funded by the FEDER Program of the European Union (“Unha maneira de facer Europa”). Dr. Beatriz Gullón would like to express her gratitude to the Spanish Ministry of Economy and Competitiveness for her postdoctoral grant (Reference RYC2018-

026177-I). Xiana Rico is thankful for her predoctoral grant (reference ED481A-2018/300) with financial support from the “Xunta de Galicia”. The authors would like to thank the Centro de Apoio Científico-Tecnolóxico á Investigación (C.A.C.T.I.) for performing the nitrogen and mineral content determination. Funding for open access charge: Universidade de Vigo/CISUG.

References

- [1] Dafnomilis I, Hoefmagels R, Pratama YW, Schott DL, Lodewijks G, Junginger M. Review of solid and liquid biofuel demand and supply in Northwest Europe towards 2030 – A comparison of national and regional projections. *Renew Sustain Energy Rev* 2017;78:31–45. <https://doi.org/10.1016/j.rser.2017.04.108>.
- [2] Hansen JP, Narbel PA, Aksnes DL. Limits to growth in the renewable energy sector. *Renew Sustain Energy Rev* 2017;70:769–74. <https://doi.org/10.1016/j.rser.2016.11.257>.
- [3] Manhongo TT, Chimphango AFA, Thornley P, Röder M. Current status and opportunities for fruit processing waste biorefineries. *Renew Sustain Energy Rev* 2022;155:111823. <https://doi.org/10.1016/j.rser.2021.111823>.
- [4] Cherubini F. The biorefinery concept: Using biomass instead of oil for producing energy and chemicals. *Energy Convers Manag* 2010;51:1412–21. <https://doi.org/10.1016/j.enconman.2010.01.015>.
- [5] European Parliament - Council of the European Union. Proposal COM/2021/557. European Parliament, Council of the European Union; 2021.
- [6] European Parliament - Council of the European Union. Directive (EU) 2018/2001. 2018.
- [7] European Parliament - Council of the European Union. Communication COM/2019/640. Brussels: 2019.
- [8] Kumar R, Tabatabaei M, Karimi K, Sárvári HI. Recent updates on lignocellulosic biomass derived ethanol – a review. *Biofuel Res J* 2016;3:347–56. <https://doi.org/10.18331/BRJ2016.3.1.4>.
- [9] Narula CK, Li Z, Casbeer EM, Geiger RA, Moses-Debus M, Keller M, et al. Heterobimetallic Zeolite, InV-ZSM-5, enables efficient conversion of biomass derived ethanol to renewable hydrocarbons. *Sci Rep* 2015;5:16039. <https://doi.org/10.1038/srep16039>.
- [10] Rajesh Banu J, Preethi, Kavitha S, Tyagi VK, Gunasekaran M, Karthikeyan OP, et al. Lignocellulosic biomass based biorefinery: A successful platform towards circular bioeconomy. *Fuel* 2021;302:121086. <https://doi.org/10.1016/j.fuel.2021.121086>.
- [11] del Río PG, Gullón B, Wu J, Saddler J, Garrote G, Romaní A. Current breakthroughs in the hardwood biorefineries: Hydrothermal processing for the co-production of xylooligosaccharides and bioethanol. *Bioresour Technol* 2022;343:126100. <https://doi.org/10.1016/j.biortech.2021.126100>.
- [12] Roukas T, Kotzekidou P. From food industry wastes to second generation bioethanol: a review. *Rev Environ Sci Bio/Technology* 2022;21:299–329. <https://doi.org/10.1007/s1157-021-09606-9>.
- [13] Salehi Jouzani G, Taherzadeh MJ. Advances in consolidated bioprocessing systems for bioethanol and butanol production from biomass: a comprehensive review. *Biofuel Res J* 2015;2:152–95. <https://doi.org/10.18331/BRJ2015.2.1.4>.
- [14] del Río PG, Domínguez VD, Domínguez E, Gullón P, Gullón B, Garrote G, et al. Comparative study of biorefinery processes for the valorization of fast-growing Paulownia wood. *Bioresour Technol* 2020;314:123722. <https://doi.org/10.1016/j.biortech.2020.123722>.
- [15] Romaní A, Larramendi A, Yáñez R, Cancela Á, Sánchez Á, Teixeira JA, et al. Valorization of *Eucalyptus nitens* bark by organosolv pretreatment for the production of advanced biofuels. *Ind Crops Prod* 2019;132:327–35. <https://doi.org/10.1016/j.indcrop.2019.02.040>.

- [16] Mallek-Ayadi S, Bahloul N, Kechaou N. Characterization, phenolic compounds and functional properties of *Cucumis melo* L. peels. *Food Chem* 2017;221:1691–7. <https://doi.org/10.1016/j.foodchem.2016.10.117>.
- [17] FAO. Faostat Database 2022. www.fao.org/faostat (accessed April 1, 2022).
- [18] Rico X, Gullón B, Alonso JL, Yáñez R. Recovery of high value-added compounds from pineapple, melon, watermelon and pumpkin processing by-products: An overview. *Food Res Int* 2020;132:109086. <https://doi.org/10.1016/j.foodres.2020.109086>.
- [19] Rolim PM, Seabra LMJ, de Macedo GR. Melon by-products: biopotential in human health and food processing. *Food Res Int* 2019;36:15–38. <https://doi.org/10.1080/87559129.2019.1613662>.
- [20] Gómez-García R, Campos DA, Aguilar CN, Madureira AR, Pintado M. Valorization of melon fruit (*Cucumis melo* L.) by-products: phytochemical and biofunctional properties with emphasis on recent trends and advances. *Trends Food Sci Technol* 2020;99:507–19. <https://doi.org/10.1016/j.tifs.2020.03.033>.
- [21] Rico X, Gullón B, Yáñez R. Environmentally friendly hydrothermal processing of melon by-products for the recovery of bioactive pectic-oligosaccharides. *Foods* 2020;9:1702. <https://doi.org/10.3390/foods9111702>.
- [22] Salehi R, Taghizadeh-Alisaraei A, Jahanbakhshi A, Shahidi F. Evaluation and measurement of bioethanol extraction from melon waste (Qassari cultivar). *Agric Eng Int CIGR J* 2018;20:127–31.
- [23] Zanivan J, Bonatto C, Scapini T, Dalastra C, Bazoti SF, Júnior SLA, et al. Evaluation of bioethanol production from a mixed fruit waste by *Wickerhamomyces* sp. UFFS-CE-312. *BioEnergy Res* 2022;15:175–82. <https://doi.org/10.1007/s12155-021-10273-5>.
- [24] Chaudhary A, Hussain I, Ahmad Q-A, Hussain Z, Akram AM, Hussain A. Efficient utilization of melon peels to produce ethanol: a step toward sustainable waste management. *Biomass Convers Biorefinery* 2022. <https://doi.org/10.1007/s13399-022-02687-8>.
- [25] Rico X, Gullón B, Yáñez R. A comparative assessment on the recovery of pectin and phenolic fractions from aqueous and DES extracts obtained from melon peels. *Food Bioprocess Technol* 2022;15:1406–21. <https://doi.org/10.1007/s11947-022-02823-2>.
- [26] Ghose TK. Measurement of cellulase activities. *Pure Appl Chem* 1987;59:257–68. <https://doi.org/10.1351/pac198759020257>.
- [27] Martínez M, Gullón B, Schols HA, Alonso JL, Parajó JC. Assessment of the production of oligomeric compounds from sugar beet pulp. *Ind Eng Chem Res* 2009;48:4681–7. <https://doi.org/10.1021/ie8017753>.
- [28] Holtzapfel MT, Caram HS, Humphrey AE. A comparison of two empirical models for the enzymatic hydrolysis of pretreated poplar wood. *Biotechnol Bioeng* 1984; 26:936–41. <https://doi.org/10.1002/bit.260260818>.
- [29] Sulieman AK, Putra MD, Abasaeed AE, Gaily MH, Al-Zahrani SM, Zeinelabdeen MA. Kinetic modeling of the simultaneous production of ethanol and fructose by *Saccharomyces cerevisiae*. *Electron J Biotechnol* 2018;34:1–8. <https://doi.org/10.1016/j.ejbt.2018.04.006>.
- [30] Blumenkrantz N, Asboe-Hansen G. New method for quantitative determination of uronic acids. *Anal Biochem* 1973;54:484–9. [https://doi.org/10.1016/0003-2697\(73\)90377-1](https://doi.org/10.1016/0003-2697(73)90377-1).
- [31] Talekar S, Patti AF, Vijayaraghavan R, Arora A. An integrated green biorefinery approach towards simultaneous recovery of pectin and polyphenols coupled with bioethanol production from waste pomegranate peels. *Bioresour Technol* 2018; 266:322–34. <https://doi.org/10.1016/j.biortech.2018.06.072>.
- [32] Kley Valladares-Diestra K, de Souza P, Vandenberghe L, Ricardo SC. A biorefinery approach for pectin extraction and second-generation bioethanol production from cocoa pod husk. *Bioresour Technol* 2022;346:126635. <https://doi.org/10.1016/j.biortech.2021.126635>.
- [33] Nolasco RX, Ascêncio SD, Ballin F, Soares IM, da Costa OJ, Nazareno JC. Influence of aluminum and magnesium in fermentation processes of hydrolyzed wastes of the banana tree for ethanol production. *Rev Em Agronegocio e Meio Ambient* 2020;13: 1533–49. <https://doi.org/10.17765/2176-9168.2020V13N4P1533-1549>.
- [34] Schwarz LV, Marcon AR, Delamare APL, Echeverrigaray S. Influence of nitrogen, minerals and vitamins supplementation on honey wine production using response surface methodology. *J Apic Res* 2020;60:57–66. <https://doi.org/10.1080/00218839.2020.1793277>.
- [35] Song W, Lagmay V, Jeong B-G, Jung J, Chun J. Changes in physicochemical and functional properties of *Opuntia humifusa* during fermentation with cellulolytic enzyme and lactic acid bacteria. *LWT* 2022;159:113192. <https://doi.org/10.1016/j.lwt.2022.113192>.
- [36] Zhang C, Zhu X, Zhang F, Yang X, Ni L, Zhang W, et al. Improving viscosity and gelling properties of leaf pectin by comparing five pectin extraction methods using green tea leaf as a model material. *Food Hydrocoll* 2020;98:105246. <https://doi.org/10.1016/j.foodhyd.2019.105246>.
- [37] Mazarei F, Jooyandeh H, Noshad M, Hojjati M. Polysaccharide of caper (*Capparis spinosa* L.) Leaf: Extraction optimization, antioxidant potential and antimicrobial activity. *Int J Biol Macromol* 2017;95:224–31. <https://doi.org/10.1016/j.ijbiomac.2016.11.049>.
- [38] Myers RH, Montgomery DC. *Response surface methodology: process and product optimization using designed experiments*. New York: Wiley; 2002.
- [39] Gullón B, Yáñez R, Alonso JL, Parajó JC. L-Lactic acid production from apple pomace by sequential hydrolysis and fermentation. *Bioresour Technol* 2008;99: 308–19. <https://doi.org/10.1016/j.biortech.2006.12.018>.
- [40] Romaní A, Garrote G, Alonso JL, Parajó JC. Experimental assessment on the enzymatic hydrolysis of hydrothermally pretreated *Eucalyptus globulus* wood. *Ind Eng Chem Res* 2010;49:4653–63. <https://doi.org/10.1021/ie100154m>.
- [41] Domínguez E, Romaní A, Domínguez L, Garrote G. Evaluation of strategies for second generation bioethanol production from fast growing biomass *Paulownia* within a biorefinery scheme. *Appl Energy* 2017;187:777–89. <https://doi.org/10.1016/j.apenergy.2016.11.114>.
- [42] Nitsos CK, Choli-Papadopoulou T, Matis KA, Triantafyllidis KS. Optimization of hydrothermal pretreatment of hardwood and softwood lignocellulosic residues for selective hemicellulose recovery and improved cellulose enzymatic hydrolysis. *ACS Sustain Chem Eng* 2016;4:4529–44. <https://doi.org/10.1021/acssuschemeng.6b00535>.
- [43] Phukoetphim N, Salakkam A, Laopaiboon P, Laopaiboon L. Kinetic models for batch ethanol production from sweet sorghum juice under normal and high gravity fermentations: Logistic and modified Gompertz models. *J Biotechnol* 2017;243: 69–75. <https://doi.org/10.1016/j.jbiotec.2016.12.012>.
- [44] Laltha M, Sewsynker-Sukai Y. Development of microwave-assisted alkaline pretreatment methods for enhanced sugar recovery from bamboo and corn cobs: Process optimization, chemical recyclability and kinetics of bioethanol production. *Ind Crops Prod* 2021;174:114166. <https://doi.org/10.1016/j.indcrop.2021.114166>.
- [45] Chohan NA, Aruwajoye GS, Sewsynker-Sukai Y, Gueguim Kana EB. Valorisation of potato peel wastes for bioethanol production using simultaneous saccharification and fermentation: process optimization and kinetic assessment. *Renew Energy* 2020;146:1031–40. <https://doi.org/10.1016/j.renene.2019.07.042>.
- [46] Dodić JM, Vučurović DG, Dodić SN, Grahovac JA, Popov SD, Nedeljković NM. Kinetic modelling of batch ethanol production from sugar beet raw juice. *Appl Energy* 2012;99:192–7. <https://doi.org/10.1016/j.apenergy.2012.05.016>.
- [47] Rohowsky B, Häbler T, Gladis A, Remmele E, Schieder D, Faulstich M. Feasibility of simultaneous saccharification and juice co-fermentation on hydrothermal pretreated sweet sorghum bagasse for ethanol production. *Appl Energy* 2013;102: 211–9. <https://doi.org/10.1016/j.apenergy.2012.03.039>.
- [48] Hamley-Bennett C, Lye GJ, Leak DJ. Selective fractionation of Sugar Beet Pulp for release of fermentation and chemical feedstocks; optimisation of thermo-chemical pre-treatment. *Bioresour Technol* 2016;209:259–64. <https://doi.org/10.1016/j.biortech.2016.02.131>.
- [49] Mazaheri D, Orooji Y, Mazaheri M, Moghaddam MS, Karimi-Maleh H. Bioethanol production from pomegranate peel by simultaneous saccharification and fermentation process. *Biomass Convers Biorefinery* 2021. <https://doi.org/10.1007/s13399-021-01562-2>.
- [50] Patsalou M, Samanides CG, Prototapa E, Stavrinos S, Vyrides I, Koutinas M. A citrus peel waste biorefinery for ethanol and methane production. *Molecules* 2019;24:2451. <https://doi.org/10.3390/molecules24132451>.
- [51] Huang R, Cao M, Guo H, Qi W, Su R, He Z. Enhanced ethanol production from pomelo peel waste by integrated hydrothermal treatment, multienzyme formulation, and fed-batch operation. *J Agric Food Chem* 2014;62:4643–51. <https://doi.org/10.1021/jf405172a>.
- [52] Tomás-Pejó E, Oliva JM, González A, Ballesteros I, Ballesteros M. Bioethanol production from wheat straw by the thermotolerant yeast *Kluyveromyces marxianus* CECT 10875 in a simultaneous saccharification and fermentation fed-batch process. *Fuel* 2009;88:2142–7. <https://doi.org/10.1016/j.fuel.2009.01.014>.